Substituent Effects on Xenon Binding Affinity and Solution Behavior of Water-Soluble Cryptophanes

4 AUTHORS, INCLUDING:

Philip Aru Hill
University of Pennsylvania
12 PUBLICATIONS   372 CITATIONS

SEE PROFILE

Thomas Troxler
University of Pennsylvania
47 PUBLICATIONS   1,218 CITATIONS

SEE PROFILE

Ivan J Dmochowski
University of Pennsylvania
80 PUBLICATIONS   1,779 CITATIONS

SEE PROFILE

Substituent Effects on Xenon Binding Affinity and Solution Behavior of Water-Soluble Cryptophanes

P. Aru Hill[†], **Qian Wei**[†], **Thomas Troxler**[‡], and **Ivan J. Dmochowski**[*,†]

Contribution from the Department of Chemistry and Regional Laser and Biotechnology Laboratories, University of Pennsylvania, Philadelphia, PA 19104

Abstract

A water-soluble triacetic acid cryptophane-A derivative (**TAAC**) was synthesized and determined by isothermal titration calorimetry (ITC) and fluorescence quenching assay to have a xenon association constant of 33,000 M^{-1} at 293 K, which is the largest value measured for any host molecule to date. Fluorescence lifetime measurements of **TAAC** in the presence of varying amounts of xenon indicated static quenching by the encapsulated xenon and the presence of a second non-xenon-binding conformer in solution. Acid-base titrations and aqueous NMR spectroscopy of **TAAC** and a previously synthesized tri-(triazole propionic acid) cryptophane-A derivative (**TTPC**) showed how solvation of the carboxylate anions can affect the aqueous behavior of the large, nonpolar cryptophane. Specifically, whereas only the crown-crown (CC) conformer of **TTPC** was observed, a crown-saddle (CS) conformer of **TAAC** was also detected in aqueous solution.

Introduction

Xenon-129 biosensors offer exciting potential for the simultaneous magnetic resonance imaging (MRI) of multiple frequency-resolved biomolecular targets. In addition to being a relatively abundant isotope of a non-toxic noble gas, the xenon-129 nucleus is spin-1/2 and can be laser-polarized to increase nuclear magnetic resonance (NMR) signals more than 10,000-fold. The polarizability of the xenon electron cloud imparts considerable environmental sensitivity to the chemical shift of the ^{129}Xe nucleus, producing a nearly 300 ppm ^{129}Xe NMR chemical shift window in common solvents.[1] This sensitivity facilitates the simultaneous detection of monatomic ^{129}Xe in different chemical environments. Biosensors exploiting this property have been generated by attaching a xenon-binding cryptophane-A moiety to protein-specific ligands such as biotin[2,3] or protease-specific peptides.[4] Cryptophane-based biosensors can be spectrally and spatially resolved in MR imaging[5–8] and a previously synthesized tri-(triazole propionic acid) cryptophane-A derivative (**TTPC,** Figure 1) was shown to be a competent xenon binder, even under near-physiological conditions.[9] The crystal structure of a benzenesulfonamide-functionalized cryptophane-A complexed with carbonic anhydrase II was solved[10] and hyperpolarized ^{129}Xe spectroscopy has demonstrated the ability of a series of the benzenesulfonamide-functionalized cryptophane-A derivatives to exhibit isozyme specific chemical shift changes upon binding to carbonic anhydrases I and II.[11] Many potential biosensing applications motivate the design and study of new xenon-binding host molecules in both organic[12–15] and aqueous phases.[13–15]

The study of gas encapsulation by host molecules remains a challenge, with few suitable analytical techniques available.[16] Recent studies of hydrocarbon gas binding by synthetic hosts in solution have relied on direct observation of the encapsulated ^{1}H NMR signals.[16,17] Even

---

*To whom correspondence should be addressed. E-mail: E-mail: ivandmo@sas.upenn.edu.

binding of gasses without proton resonances such as Ar, CO, O_2, and N_2 by self assembled oxime capsules in chloroform have been studied by ^{1}H NMR spectroscopy.[18] In the solid phase, single crystals of calix[4]arene have been shown to store gaseous guest molecules with high thermal stability.[19] Elegant studies of NO, air, SO_2, and xenon adsorbtion by the Ripmeester lab have demonstrated that *p-tert*-butylcalix[4]arene host molecules are capable of creating discreet gas binding spaces in the solid state.[20,21] Xenon binding to the host cavities in amphiphilic calixarene-based solid lipid nanoparticles has also been studied through the use of continuous flow hyperpolarized [129]Xe MAS NMR.[22] While solution NMR has proven to be useful in the direct determination of association constants from $10\text{-}10^4 \text{ M}^{-1}$, competition experiments are necessary to measure greater affinities.[23] Fluorescence spectroscopy and isothermal titration calorimetry (ITC) allow for the direct detection of binding equilibria at micromolar concentrations of analyte. These techniques can be applied to host-gas chemistry through the controlled addition of saturated gas solutions of known concentration, as previously demonstrated for xenon.[9]

In this study a new water-soluble xenon-binding host, triacetic acid cryptophane-A (**TAAC**) was synthesized and compared to the previously synthesized **TTPC** (Figure 1).[9] **TAAC** and **TTPC** each have a tri-substituted cyclotriveratrylene (CTV) moiety, which differs in the linkage to three carboxylates. Although the cryptophane core of **TAAC** and **TTPC** is identical, **TAAC** was shown by NMR and pH titration to exhibit different solution-phase behavior. **TAAC** also exhibited roughly 2-fold higher affinity for xenon, as measured by fluorescence quenching assay and ITC. Both **TAAC** and **TTPC** were studied by time-correlated single-photon counting (TCSPC), which confirmed static fluorescence quenching by the encapsulated xenon. These studies demonstrate that the solubilizing groups appended to otherwise identical cryptophane cores can have a significant effect on molecular conformation and xenon-binding. This provides new insight into the aqueous phase behavior of the cryptophane component of known xenon biosensors.

Experimental Procedures

Reagents

Organic reagents and solvents were used as purchased from the following commercial sources: Acros: cesium carbonate, anhydrous dimethylsulfoxide (DMSO), anhydrous dimethylformamide (DMF), d_6-DMSO, $CDCl_3$, 4-hydroxy-3-methoxybenzylalcohol, triphenylphosphine, 1,2 dibromoethane, sodium borohydride, 10% palladium on carbon, 3,4-dihydroxybenzaldhyde, ethyl bromoacetate, palladium(II) acetate. Fisher: sodium chloride, potassium phosphate, ethyl acetate, dichloromethane, chloroform, hydrochloric acid, sodium hydroxide, sodium sulfate, acetone, hexanes, sodium iodide, potassium hydroxide. Cambridge Isotope Laboratories: deuterium oxide. Airco Industrial Gases: research grade xenon gas. Aldrich: 3,4-dihydro-2H-pyran, allyl bromide, pyridinium *p*-toluenesulfonate, sodium deuteroxide 40 wt.% in D_2O, diethylamine.

General Methods

All organic reactions were carried out under nitrogen atmosphere. ^{1}H NMR (500.14 MHz) and [13]C (125.77 MHz) spectra were obtained on a Bruker AMX 500 or DMX 600 spectrometer at the University of Pennsylvania NMR Facility. Spectra were referenced to TMS at 0.00 ppm in $CDCl_3$ or the residual solvent peak at 2.50 ppm in d_6-DMSO. Electrospray ionization (ESI) mass spectrometry was performed in low-resolution mode on a Micromass LC Platform and in high-resolution mode on a Micromass Autospec at the Mass Spectrometry Center in the Chemistry Department at the University of Pennsylvania. For fluorescence and ITC measurements in buffer, solutions were prepared with water deionized using Mar Cor Premium Grade Mixed Bed Service Deionization. Column chromatography was performed using 60 Å

porosity, 40–75 µm particle size silica gel form Sorbent Technologies. Thin layer chromatography was performed using silica gel plates with UV light at 254 nm for detection.

2,7,12-Tris(2-[2-allyloxy-4-[tetrahydro-pyran-2-yloxymethyl]-phenoxyl]-ethoxy)-3,8,13-trimethoxy-10,15-dihydro-5H-tribenzo[*a,d,g*]cyclononene (3)

2 (1.460 g, 3.575 mmol) and cesium carbonate (6.98 g, 21.45 mmol) were added to an oven-dried flask with stir bar and purged with nitrogen gas. Dry DMF (150 mL) was added by syringe and the mixture was allowed to stir for 30 min at rt. Linker **1** (5.981 g, 14.30 mmol) was then added and the reaction was placed in a 55 °C oil bath with stirring overnight. The reaction was poured into saturated NaCl (600 mL), and extracted 3 times with Et$_2$O (300 mL). The combined organics were washed 5 times with saturated NaCl (300 mL), dried over Na$_2$SO$_4$, and evaporated under reduced pressure. The crude material was then pumped under high vacuum to remove any residual DMF and purified by column chromatography (CH$_2$Cl$_2$ → 90:10 CH$_2$Cl$_2$:acetone) to obtain **3** (2.74 g, 60% yield) as a clear glass. ^{1}H NMR (CDCl$_3$) δ = 6.98 (s, 3H, aryl), 6.94-6.87 (m, 9H, aryl), 6.83 (s, 3H, aryl), 6.04 (m, 3H, allyl), 5.38 (m, 3H, allyl), 5.22 (m, 3H, allyl), 4.73 (d, 3H, H$_{ax}$, J = 13.6 Hz), 4.69 (d, 3H, Ph-CH_2-O, J = 11.8 Hz), 4.67 (t, 3H, THP), 4.59 (d, 6H, allyl), 4.38 (d, 3H, Ph-CH_2-O, J = 11.8 Hz), 4.35 (m, 12H, O-CH_2-CH_2-O), 3.91 (m, 3H, THP), 3.74, (s, 9H, O-CH_3), 3.53 (m, 3H, THP), 3.53 (d, 3H, H$_{eq}$, J = 13.5 Hz), 1.88-1.49 (m, 18H, THP). ^{13}C NMR (CDCl$_3$) δ = 148.62, 148.51, 148.08, 146.79, 133.44, 132.91, 131.81, 131.74, 120.87, 117.27, 116.64, 114.62, 114.50, 114.01, 97.38. 69.92, 68.40, 68.21, 67.90, 61.99, 56.12, 36.18, 30.47, 25.35, 19.30. HRMS calcd for C$_{75}$H$_{90}$O$_{18}$ (M + Na$^+$) 1301.6025, found 1301.6015.

Tri-Allyl Cryptophane (4)

3 (560 mg, 0.39 mmol) was dissolved in 250 mL CHCl$_3$ and 250 mL formic acid was added with magnetic stirring. The reaction was purged with N$_2$ before being heated to reflux for 9 h. The solvent was then evaporated under reduced pressure. Toluene was added to the crude material and evaporated under reduced pressure to remove residual formic acid. The crude material was then purified by column chromatography (CH$_2$Cl$_2$ → CH$_2$Cl$_2$:diethyl ether 90:10) to obtain **4** (152 mg, 40% yield). ^{1}H NMR (CDCl$_3$) δ = 6.76 (s, 3H, aryl), 6.74 (s, 3H, aryl), 6.72 (s, 3H, aryl), 6.67 (s, 3H, aryl), 6.05 (m, 3H, allyl), 5.45 (m, 3H, allyl), 5.34 (m, 3H, allyl), 4.59 (d, 3H, H$_{ax}$, J = 13.9 Hz), 4.55 (d, 3H, H$_{ax}$, J = 13.7 Hz), 4.49 (m, 6H, allyl), 4.16 (m, 12 H, O-CH_2-CH_2-O), 3.74 (s, 9H, O-CH_3), 3.40 (d, 3H, H$_{eq}$, J = 13.5 Hz), 3.37 (d, 3H, H$_{eq}$, J = 13.4 Hz). ^{13}C NMR (CDCl$_3$) δ = 149.95, 149.21, 147.53, 146.96, 134.53, 134.36, 134.02, 132.51, 131.91, 122.35, 120.94, 117.17, 116.89, 114.47, 70.27, 69.83, 69.58, 56.48, 36.43. HRMS calcd for C$_{60}$H$_{60}$O$_{12}$ (M + MeCN + Na$^+$) 1036.4248 found 1036.4261.

Tri-OH Cryptophane (5)

4 (303 mg, 0.31 mmol), triphenylphosphine (135 mg, 0.51 mmol), palladium acetate (7.7 mg, 0.03 mmol), diethylamine (1.5 g, 20.5 mmol), THF (4.8 mL), and water (0.95 mL) were added to a screw-capped high-pressure tube. The tube was purged with nitrogen, sealed, and placed in an 80 °C oil bath with magnetic stirring for 4 h. After cooling to rt, the solvent was removed by evaporation under reduced pressure. The crude material was dissolved in CH$_2$Cl$_2$ (100 mL), washed twice with 1 M HCl (50 mL) and once with saturated NaCl (50 mL). The crude material was then adsorbed onto silica gel and purified by column chromatography (CH$_2$Cl$_2$ → 80:20 CH$_2$Cl$_2$:acetone) to obtain **5** (220 mg, 84% yield) as a white solid. ^{1}H NMR (DMSO-d_6) δ = 8.50 (s, 3H, Ar-OH), 6.83 (s, 3H, aryl), 6.77 (s, 3H, aryl), 6.60 (s, 3H, aryl), 6.53 (s, 3H, aryl), 4.50 (d, 3H, H$_{ax}$, J = 13 Hz) 4.40 (d, 3H, H$_{ax}$, J = 13 Hz), 4.20-4.00 (m, 12H, O-CH_2-CH_2-O), 3.73 (s, 9H, Ar-OCH_3), 3.31 (d, 3H, H$_{eq}$, J = 14 Hz), 3.15 (d, 3H, H$_{eq}$, J = 14 Hz). ^{13}C NMR (DMSO-d_6) δ = 148.91, 146.59, 145.81, 144.29, 133.79, 133.33, 131.15, 129.58, 120.62,

120.10, 117.45, 114.22, 68.50, 55.72, 35.03. HRMS calcd for $C_{51}H_{48}O_{12}$ (M+Na$^+$) 875.3043, found 875.3053.

Tri-EtOAc Cryptophane (6)

5 (189 mg, 0.22 mmol) and cesium carbonate (0.43 g, 1.3 mmol) were added to an oven-dried flask with stir bar and purged with nitrogen gas. Dry DMF (5 mL) was added by syringe and the mixture was allowed to stir for 30 min at rt. Ethyl bromoacetate (0.22 g, 1.33 mmol) was then added and the reaction was placed in a 60 °C oil bath with stirring overnight. The DMF was removed by evaporation under reduced pressure. The crude reaction mixture was dissolved in CH_2Cl_2 (50 mL), washed with saturated NaCl (50 mL), dried over Na_2SO_4, and evaporated under reduced pressure. The crude material was then pumped under high vacuum to remove any residual DMF and purified by column chromatography ($CH_2Cl_2 \rightarrow$ 80:20 CH_2Cl_2:diethyl ether) to obtain **6** (0.194 g, 79% yield) as a white solid. ^{1}H NMR (CDCl$_3$) δ =6.76 (s, 3H, aryl), 6.75 (s, 3H, aryl), 6.71 (s, 3H, aryl), 6.69 (s, 3H, aryl), 4.58 (d, 3H, H$_{ax}$, J = 14 Hz), 4.55 (d, 3H, Ar-O-CH_2-CO$_2$, J = 16 Hz), 4.54 (d, 3H, H$_{ax}$, J = 14 Hz), 4.50 (d, 3H, Ar-O-CH_2-CO$_2$, J = 16 Hz), 4.32-4.19 (m, 18H, O-CH_2-CH_2-O, CO$_2$-CH_2-CH$_3$), 3.76 3.67 (s, 9H, Ar-OCH_3), 3.40 (d, 3H, H$_{eq}$, J = 14 Hz) 3.38 (d, 3H, H$_{eq}$, J = 14 Hz), 1.35 (t, 9H, CH2-CH_3, J = 7 Hz). ^{13}C NMR (CDCl$_3$) δ = 168.74, 149.73, 148.02, 147.73, 146.79, 134.02, 133.95, 133.73, 131.79, 121.88, 120.62, 118.18, 114.71, 69.56, 69.24, 67.20, 61.20, 56.21, 36.20, 36.11, 14.34 HRMS calcd for $C_{63}H_{66}O_{18}$ (M + Na$^+$) 1133.4147, found 1133.4134.

Tri-Acid Cryptophane (TAAC)

6 (194 mg, 0.17 mmol), 2 M KOH (7.35 mL), and THF (8.75 mL) were added to a screw-capped high-pressure tube. The tube was purged with nitrogen, sealed, and placed in a 70 °C oil bath with magnetic stirring overnight. The THF was then removed by evaporation under reduced pressure. The aqueous solution was transferred to a centrifuge tube, acidified with 12 M HCl and centrifuged. The solid pellet was redissolved in 1 M NaOH, acidified with 12 M HCl and centrifuged. The solid pellet was then dispersed in deionized water, centrifuged, and the water decanted. After lyophilization of the resulting pellet, 0.1559 g of **TAAC** was obtained in 87% yield. ^{1}H NMR (DMSO-d_6) δ = 6.85 (s, 3H, aryl), 6.83 (s, 3H, aryl), 6.82 (s, 3H, aryl), 6.77 (s, 3H, aryl), 4.54 (s, 6H, Ar-O-CH_2-CO$_2$), 4.48 (d, 6H, H$_{ax}$, J = 13 Hz), 4.06–4.25 (m, 12H, O-CH_2-CH_2-O), 3.67 (s, 9H, Ar-OCH_3), 3.31 (d, 3H, H$_{eq}$, J = 13 Hz), 3.28 (d, 3H, H$_{eq}$, J = 13 Hz). ^{13}C NMR (d_6-DMSO) δ = 170.16, 148.75, 147.173, 145.60, 133.55, 133.45, 132.42, 131.69, 120.41, 118.95, 115.86, 114.96, 68.64, 68.17, 65.49, 55.87, 34.88. HRMS calcd for $C_{57}H_{54}O_{18}$ (M + Na$^+$) 1049.3208, found 1049.3211.

Isothermal Titration Calorimetry

ITC samples were prepared and experiments were performed as previously described[9] using a MicroCal VP-ITC titration microcalorimeter (Northampton, MA) at 293 K. Standard protocols and data analysis were used.[24,25] Control enthalpograms are given in the Supporting Information (Figure S1).

Steady-State Fluorescence

Steady-state fluorescence spectra were acquired using a Varian Cary Eclipse fluorimeter equipped with a Peltier multicell holder for temperature control. Concentration measurements necessary for fluorescence work were obtained using an Agilent 8453 UV-Vis spectrophotometer. Xenon binding determination by fluorescence quenching was performed on 15 µM solutions of **TAAC** or **TTPC**, as previously described.[9] The following single-site binding model was used:

$$\frac{[\text{Xe@Cr}]}{[\text{Cr}]+[\text{Xe@Cr}]}=\frac{[\text{Xe}]}{[\text{Xe}]+1/K_A}$$

(1)

where the left side of Eq. 1 indicates the fraction of cryptophane (*Cr*) in solution that is bound by xenon, and K_A is the xenon association constant.

The quantum yields of **TAAC** and **TTPC** in 0.001 M, pH 7.2 phosphate buffer were measured relative to tryptophan.[26]

Aqueous ^{1}H NMR Spectroscopy

Solutions (180 mM) were made by deprotonation of 0.011 mmol **TAAC** and **TTPC** using sodium deuteroxide 40 wt.% in D_2O and subsequent dissolution in 600 µL of 10% D_2O/H_2O. These samples were transferred to 5-mm controlled atmosphere valve sample tubes (New Era Spectroscopy) to allow for degassed- and xenon-saturated ^{1}H NMR spectroscopy.

Time-resolved Fluorescence

Time-resolved fluorescence measurements were performed at 293 K using the TCSPC method. The TCSPC system consisted of the third harmonic of a Ti:sapphire femtosecond laser (Coherent Chameleon) generating 80 MHz output pulses at 275 nm, a subtractive double monochromator with a MCP-PMT (Hamamatsu R2809U) and a TCSPC board (Becker & Hickl, SPC-730). Emission at 310 nm was monitored. Data analysis was done using the FLUOFIT software (Picoquant GmbH). Fluorescence decays were deconvolved with an instrument response function of 35 ps and globally fit using a three exponential model.

Results

Synthesis

TAAC was synthesized (Scheme 1) by a modification of the synthesis of monoallyl-cryptophane by Darzac et al.[27,28] Cyclotriveratrylene **1** in DMF was deprotonated with cesium carbonate and reacted with 4.5 equiv 2-[3-allyloxy-4-(2-iodo-ethoxy)-benzyloxy]-tetrahydropyran **2** at 55 °C in 60% yield to obtain **3**.

In 50:50 chloroform:formic acid, the cyclization of **3** proved extremely slow at 55 °C and higher temperatures were necessary to push the reaction beyond a partially cyclized intermediate. It is hypothesized that the three allyl groups provided steric hindrance that allowed the observation of this intermediate. An optimum reaction time of 9 h at reflux was found (Table 1) to give triallyl-cryptophane **4** in 40% yield, compared to 2.5 h at 55 °C for monoallyl-cryptophane.[28] Use of a higher boiling solvent system, 50:50 1,2-dichloroethane:formic acid, led to decomposition of **3**. The cyclized product **4** is known to be of the *anti* isomer, as confirmed by its X-ray crystal structure with chloroform as an encapsulated guest.[29]

Deprotection of **4** to the triphenol-cryptophane **5** was accomplished in 84% yield by palladium catalysis using known procedures.[30] The triphenol **5** was then triply alkylated using ethylbromoacetate and cesium carbonate in DMF to give triester-cryptophane **6** in 79% yield. Saponification of **6** in THF using potassium hydroxide produced **TAAC** in 87% yield. The conversion of starting 3,4-dihydroxybenzaldehyde to **TAAC** occurred in 13 steps in 1.7% overall yield with a longest linear sequence of 10 steps.

Binding of Xenon by TAAC

The xenon affinity of **TAAC** was studied by fluorescence quenching (Figure 2) and ITC (Figure 3). An extinction coefficient of 12,040 $M^{-1}cm^{-1}$ at 280 nm was determined for **TAAC**, which varied only slightly from the previously determined value of ε_{280} = 12,400 $M^{-1}cm^{-1}$ for **TTPC**.[9] As in the previous fluorescence quenching study with **TTPC**, temperature-equilibrated solutions of xenon-saturated water were added sequentially by syringe to a septum-sealed fluorescence cuvette and fluorescence intensity measurements were taken.[9] An association constant of 33,000 ± 2000 M^{-1} at 293 K was obtained for **TAAC** by this method. No measurable change in the absorption spectrum of either **TAAC** or **TTPC** was observed upon xenon binding.

In order to confirm the association constants obtained by fluorescence quenching, ITC experiments were performed. ITC was used previously to determine the xenon binding affinity for **TTPC**[9] and more recently for a water-soluble cucurbit[6]uril derivative.[31] ITC measurements were performed at 293 K on 0.77 mM **TAAC** in 20 mM, pH 7.5 phosphate buffer (Figure 2), which gave a ΔH of −4.3 ± 0.7 kcal*mol^{-1}. From these data, ΔS of 5.9 cal*mol^{-1}*K^{-1} and ΔG of −6.09 kcal*mol^{-1} were calculated. The xenon association constant determined for **TAAC** at 293 K, K_A = 33,000 ± 3000 M^{-1}, was virtually identical to the value determined by steady-state fluorescence assay, and was significantly larger than that determined previously for **TTPC**, K_A = 17,000 ± 2000 M^{-1}.[9] Thermodynamic parameters for **TAAC** and **TTPC** are compared in Table 2.

Fluorescence Spectroscopy

The room-temperature fluorescence spectra of **TAAC** and **TTPC** consisted of a broad band with a maximum at 313 nm in phosphate buffer, similar to the 1,2-dialkoxybenzene chromophores that form the cryptophane.[32] **TAAC** exhibited a higher quantum yield than **TTPC** (Φ_f = 0.06 vs. 0.01 at 293 K). The emission of both molecules was partially quenched by ambient oxygen, implying weak oxygen binding. Because the only chemical difference between **TAAC** and **TTPC** is the nature of the pendant solubilizing groups, the lower quantum yield of **TTPC** could be explained by excited-state quenching by the three triazole rings appended to its cryptophane core. The quantum yield of **TAAC** is also temperature dependent, with a linear decrease of 0.0007/K between 283 and 313 K (Figure S2, Supporting Information). This temperature dependence is attributed to the increase in molecular motions and accessibility of different cage conformations as the thermal energy of the cryptophane system is increased.

Xenon has been shown to quench fluorescence by promoting intersystem crossing from the first singlet excited state of a chromophore (S_1) to the lowest triplet state (T_1).[33] Xenon quenching of cryptophane fluorescence is necessarily static in nature as the xenon atom is encapsulated within the chromophore assembly of the cryptophane cage, forming a complex between the fluorophores and quencher. The fluorescence quenching of **TAAC** and **TTPC** by xenon was plotted using the Stern-Volmer equation for static quenching:[34]

$$\frac{F_0}{F} = 1 + K_s[\text{Xe}]$$

(2)

Where F_o is the fluorescence intensity without xenon, F is the fluorescence intensity in the presence of xenon, K_S is the static quenching constant. If quenching is complete upon xenon encapsulation by the cryptophane, then the Stern-Volmer plot of xenon quenching cryptophane fluorescence is linear and the slope of the fitted line is equivalent to the association constant of xenon for the cryptophane:

$$K_s = \frac{[\text{Xe@Crypt}]}{[\text{Xe}][\text{Crypt}]}$$

(3)

However, in the Stern-Volmer plots for **TAAC** and **TTPC** (Figure 4), a linear correlation is observed only at low xenon concentrations, with a deviation from linearity towards the x-axis at higher xenon concentrations. At xenon saturation, maxima are achieved of $F_0/F = 6$ for **TAAC** and $F_0/F = 2$ for **TTPC**. Fits to the initial linear sections of the plots give apparent Stern-Volmer quenching constants, K_s, of 19,300 M^{-1} and 4,700 M^{-1}, respectively, for encapsulated xenon quenching (Figure 5). Horizontal deviations in Stern-Volmer plots are normally observed when there is hindered access to a particular population of fluorophores in a sample, for example a buried tryptophan residue in a protein.[34] While it may be conceivable that a co-encapsulated water molecule could prevent xenon from contacting one or more of the six 1,2-dialkoxybenzene chromophores of the cryptophane cores of **TAAC** and **TTPC**, aqueous NMR measurements provide no evidence of encapsulated water, even under degassed conditions (*vide infra*).

TCSPC measurements of the fluorescence lifetimes of **TAAC** and **TTPC** were undertaken in an effort to understand the nature of the xenon quenching and the horizontal deviation from linearity in the steady-state Stern-Volmer plots.[12] The low quantum yield and short lifetime of **TTPC** allowed only mono-exponential tailfits to be obtained, giving lifetimes of ~300 ps without encapsulated xenon and ~200 ps when saturated with xenon (Figure S3, Supporting Information).

The higher quantum yield of **TAAC** allowed for decay fits deconvolved from the TCSPC instrument response function. Rigorously purified **TAAC** in aqueous solution exhibited a double exponential decay (Figure 6 and Table 3), which was fitted to two exponentials with lifetimes of 1.1 ns (95% of total intensity) and 0.3 ns (5% of total intensity). The smaller amplitude, shorter-lived component is consistent with the presence of a second, minor conformer in solution. This minor conformer is assigned to be the non-xenon-binding crown-saddle (CS) conformer of **TAAC**. By comparison, the lifetime of the related chromophore, 1,2-dimethoxybenzene is monoexponential with a lifetime of 1.4 ns.[32] With xenon encapsulation by **TAAC**, a very short-lived component with lifetime of 0.13 ns replaced the 1.1 ns lifetime component.

Stern-Volmer analysis of the average fluorescence lifetimes of **TAAC** with encapsulated xenon was performed using the following relationship:[35]

$$\frac{\langle \tau \rangle_0}{\langle \tau \rangle} = 1 + K_{sv}^{\tau}[\text{Xe}]$$

(4)

where a fit to the initial linear section of the plot gives an apparent time–resolved Stern-Volmer quenching constant, K_{sv}^{τ}, of 2,200 M^{-1} for encapsulated xenon quenching (Figure 7). As in the steady-state Stern-Volmer plot for **TAAC**, a linear correlation is observed at low xenon concentrations with a deviation from linearity towards the x-axis at higher xenon concentrations approaching a maximum at $\tau_0/\tau = 4.6$ for **TAAC** upon xenon saturation. Because $K_{sv}^{\tau} < K_s$, it is apparent that analysis of the shorter 0.13 ns decay component associated with xenon encapsulation is necessary.

A three-exponential global fit of the lifetime data with increasing xenon occupancy was performed and the relative intensities of the three observed lifetimes are given in Table 3. The amplitude of the 0.34 ns component remained constant at 12–14% of the total initial amplitude

in the fit, indicating that this species, assigned to the CS conformer, did not take part in the xenon-binding equilibrium. At the concentrations involved, the contribution of collisional quenching between non-encapsulated xenon and the S_1 state of **TAAC** is expected to be negligible. The Einstein-Smoluchowski equation for diffusion:

$$\left\langle \overline{x}^2 \right\rangle^{1/2} = (2D\tau)^{1/2}$$

(5)

using the diffusion coefficient (D) of xenon in water ($2.2 \pm 0.4 * 10^{-5}$ cm^2 s^{-1})[36] and the short timescale of the fluorescence decays ($\tau = 1.1$ ns) predicts a root-mean-square distance of 20 Å that aqueous xenon can travel during the **TAAC** S_1 excited state. Even at the highest Xe concentrations (5 mM) investigated in these fluorescence experiments, collisional quenching from non-encapsulated xenon is not expected to contribute to the observed fluorescence quenching. From the fluorescence lifetime and quantum yield measurements of **TAAC** with no encapsulated xenon, a natural lifetime (τ_n) of 18 ns and its reciprocal emissive rate (Γ) of $5.5*10^7$ s^{-1} were calculated from the following relationship:

$$\tau_n = \frac{\tau}{\Phi_f}$$

(6)

A nonradiative decay rate (k_{nr}) of $8.5*10^8$ s^{-1} was obtained from Eq. 6:

$$k_{nr} = \frac{1}{\tau} - \Gamma$$

(7)

From the lifetime of **TAAC** in aqueous solution saturated with xenon ($\tau_{Xe} = 130$ ps), an apparent first-order quenching rate constant for the encapsulated xenon atom quenching the fluorescence of **TAAC**, $k_{Xe} = 6.8*10^9$ s^{-1}, was then computed from Eq. 7:

$$k_{Xe} = \frac{1}{\tau_{Xe}} - \Gamma - k_{nr}$$

(8)

As discussed in the work of Webber,[35] static quenching is a formalism in which the fluorophore-quencher complex is assumed to be an entirely dark state. In this instance, ultrafast techniques allow for the deconvolution of not only the lifetime of the **Xe@TAAC** complex, but also of the contribution to observed fluorescence intensity of the non-xenon-binding CS conformer of **TAAC**. TCSPC data show a minor population of **TAAC** (~5%) with a shorter lifetime than the dominant CC conformer. These observations are summarized in a modified static quenching scheme (Scheme 2) in which the effect of adding xenon to a solution of **TAAC** converts the population from the more emissive "empty" **TAAC*** excited state to a population of less emissive **Xe@TAAC***, as governed by the xenon binding affinity of **TAAC**.

Acid-Base Titration

Acid-base titrations of **TAAC** and **TTPC** (Figures S4, S5, Supporting Information) were performed in order to understand the solubility requirements and anion stabilities of the two cryptophanes. **TAAC** exhibited a pK_a of 4.1, compared to the reported pK_a of 3.23 for the analagous 2-(2-methoxyphenoxy)acetic acid.[37] Previous studies of sterically congested acetic acid derivatives have shown pK_a differences of similar magnitude, up to 1.5 pK_a units.[38] Steric

congestion near the carboxylic acid group decreases acidity by preventing efficient solvation of the carboxylate anion. For compound **TAAC**, this is due to the nonpolar surface of the ~1 nm diameter cryptophane interfering with the solvation of the three acetate anions. The nonpolar cryptophane surface must order surrounding water molecules and carboxylate solvation must compete directly with this ordered solvation sphere. In addition, based on visual observations of precipitation during the titrations, it was found that **TAAC** required all three acids to be deprotonated for aqueous solubility whereas **TTPC** required only two deprotonations for solubility to 200 μM.

The carboxylate groups of **TTPC** are ~5 Å farther from the cryptophane core and more easily stabilized through solvation. Titration of **TTPC** under the same conditions as **TAAC** yielded a pK_a of 5.3. The pK_a difference between **TTPC** and the analogous propanoic acid (pK_a = 4.87) [39] is less than one-half of a pK_a unit, indicative that the carboxylates on **TTPC** experience less effect from the bulk of the nonpolar cryptophane. Propanoic acid is relevant for comparison to **TTPC** as the triazoles on **TTPC** are greater than two methylenes from the acid groups and not expected to contribute electrostatically to their acidity. However, the dipole moments and hydrogen-bond accepting abilities of the three triazoles appended to **TTPC** are expected to aid water solubility.

Aqueous NMR Spectroscopy

In order to bind xenon, the cryptophanes in this study must exist in a C_3-symmetric crown-crown (CC) conformation, in which both CTV units adopt a concave form to create a molecular cavity. However, it was shown in the work of Huber et al[40] that water-soluble cryptophanes are capable of existing in multiple conformations in aqueous solution. Specifically, a crown-saddle (CS) conformation was proposed, in which one of the two CTV units of the cryptophane is in an asymmetric "saddle" conformer. The CTV unit possessing the saddle conformer has been proposed to fill the cavity of the cryptophane, preventing xenon binding.

In order to investigate the possible presence of a CS isomer, NMR studies of **TAAC** and **TTPC** were undertaken at 300 K in aqueous 10% D_2O solutions. The spectra of both compounds before degassing exhibited broad linewidths, particularly in the aromatic and ethylene linker resonances. This is attributed to the cryptophane being able to bind weakly gasses such as oxygen and nitrogen. While it is expected that both **TAAC** and **TTPC** are capable of binding water, no resonance was observed for either compound that could be attributed to encapsulated water (Figure 8 and Figure 9). Bound water molecules have been observed in cucurbiturils[41] and the entropic penalty of encapsulating water has been suggested to explain the observation of CS conformers of other water-soluble cryptophanes.[40] Degassing the solution with several cycles of pumping under static vacuum sharpened the aromatic and ethylene linker resonances. Saturation of the solution with xenon further sharpened all of the cryptophane core proton signals for the compounds. Similar sharpening of proton resonances upon aqueous guest encapsulation has been observed for a hexa-acid cryptophane-A derivative upon addition of chloroform.[42]

It should be noted that in **TTPC** the protons farthest from the cryptophane core exhibit sharp linewidths (N-CH$_2$ protons FWHM = 3 Hz for all three conditions) that are not affected by the nature of the various gaseous guest molecules (Figure 8). Because the cryptophane core is chiral (a mixture of M_o and P_o enantiomers)[43] the protons on the methylene connecting the cryptophane to the triazole ("H$_{Bz}$" in Figure 8) are diastereotopic, their resonances separated by 0.04 ppm and geminally splitting each other by 12 Hz upon xenon saturation. Most notably, however, no population of conformers other than the canonical CC form was detected for **TTPC**.

The degassed aqueous NMR spectrum of **TAAC** indicated less than 5% population, by NMR integration, of a second species that is consistent with the CS conformer (Figure 9). In addition to the aromatic peaks that are a result of the C_1 symmetry of the CS conformer, the bridging methylene group peaks at 0.0 and 2.0 ppm (Figure S6, Supporting Information) that correspond to the CH_2 protons pointing into the cavity are in agreement with the observations of Huber et al.[40] These peaks are not impurities as the ^{1}H NMR of **TAAC** in d_6-DMSO (molecular charge = 0, Figure S7, Supporting Information) shows only CC conformer without the need for degassing or xenon saturation. Another striking feature of **TAAC** in aqueous solution is the magnitude of diastereotopic chemical shift difference evident in the protons on the methylenes connecting the cryptophane to the carboxyl groups ("H_{Ac}" in Figure 9). These protons, as confirmed by 2-D COSY (Figure S8, Supporting Information), had resonances separated by 0.20 ppm with 15 Hz geminal splitting. This large difference in chemical shift between the two methylene protons is indicative of two very different chemical environments. When the free acid of **TAAC** was dissolved in d_6-DMSO, the H_{Ac} methylenes appeared as a singlet (Figure S7), with no apparent difference in their chemical environment. This dependence of chemical shift on the solvent and protonation state of **TAAC** supports the hypothesis that the diastereotopism observed in aqueous solution is a result of the carboxylate anions being unable to access many conformations that could produce magnetic equivalence of the protons. Adopting such conformations would lead to a loss in solvating water molecules and destabilize the three anions. It is hypothesized that the more compact CS conformer allows for more efficient solvation of the carboxylates, thermodynamically stabilizing this structure and allowing for its observation. We have not identified conditions in which the CS conformation predominates in aqueous solution.

The NMR and titration data lead us to hypothesize that the CS conformer population of **TAAC** is caused by the three deprotonated carboxylates being poorly solvated due to their close proximity to the cryptophane core. This poor anion solvation destabilizes the CC conformer. The greater salvation gained through adoption of the CS conformer allows for the observation of both conformers in aqueous solution. The carboxylates of **TTPC**, being farther away from the cryptophane core, are more efficiently solvated, which eliminates the gain in solvation that appears to be associated with adopting the more compact CS conformation.

Discussion

Given the low millimolar solubility of xenon in blood and tissue at physiological temperature, [44] host molecules capable of binding and localizing dissolved xenon at micromolar concentrations are necessary for in vivo studies. A xenon-binding host molecule in biological media must outcompete xenon partitioning into nonpolar spaces such as cell membranes and fatty tissue. For these reasons, high-affinity xenon-binding molecules will be important for the development of functional xenon NMR biosensors and other xenon-based imaging agents. Finally, the construction of target-specific xenon biosensors requires the appendage of one or more bioactive moieties to a xenon-binding host molecule. This work demonstrates that the nature of the groups appended to a cryptophane can have a significant effect on cryptophane aqueous behavior and xenon binding affinity.

Time-correlated single photon counting confirmed static quenching by the encapsulated xenon and a quenching model has been proposed to explain why only partial fluorescence quenching is observed at xenon saturation. Xenon was found to be a better fluorescence quencher of **TAAC** than **TTPC**, based on the longer fluorescence lifetime of **TAAC**. The encapsulated xenon atom occupies almost half the volume of the cryptophane cavity and presumably collides hundreds of times with each chromophore before the $S_1 \rightarrow S_0$ electronic transition occurs from the excited 1,2-dialkoxybenzene units of the cryptophane; and yet, the xenon does not completely quench the cryptophane fluorescence. Fluorescence quenching experiments

provided a useful method for determining xenon binding constants at low micromolar concentrations (15 µM) of **TAAC** or **TTPC** in buffer solution, and gave excellent agreement with ITC measurements, which were typically performed at much higher concentrations (770 µM). Despite this discrepancy, both techniques are more sensitive than typical NMR measurements, and ITC offers advantages for obtaining thermodynamic parameters and making measurements in optically dense media such as plasma.[9] The ability to prepare and handle saturated xenon solutions enabled the titration of specific quantities of xenon for the determination of xenon binding constants by both fluorescence and ITC methods.

NMR experiments indicated that **TTPC** exists only as the CC conformer in aqueous solution. Although **TAAC** exists primarily as the CC conformer in aqueous solution, resonances were also observed that correspond to a minor population ($< 5\%$) of the CS conformer. This was consistent with TCSPC data showing a minor population of **TAAC** ($\sim 5\%$) with a shorter lifetime than the dominant CC conformer. Acid-base titration data showed destabilization of the carboxylate anions of both compounds by the nonpolar cryptophane core in aqueous solution. This destabilization is hypothesized to be the driving force for the assumption of the CS conformer by **TAAC** in aqueous solution.

Conclusion

We conclude that **TAAC** exhibits the highest affinity for xenon of any known host molecule, $K_A = 33,000$ M^{-1} at 293 K. The agreement between the fluorescence quenching and ITC data further validates the use of both techniques for the determination of xenon binding constants. Although the exact origin of the -0.37 kcal/mol additional stabilization of the **Xe@TAAC** complex relative to **Xe@TTPC** at 293 K is not known, this observation demonstrates that differently functionalized cryptophane cores can lead to different xenon binding affinities. All other effects being equal, we hypothesize that introducing ionizable groups close to the cryptophane that create a molecular dipole moment within the cavity can lead to improvements in xenon binding. Solvation effects may also serve to modulate more subtly the size of the CC conformer, leading to changes in binding affinity.

Supplementary Material

Refer to Web version on PubMed Central for supplementary material.

Acknowledgment

References

1. Raftery D. Annu. Rep. NMR Spectros 2006;57:205–270.

2. Spence MM, Rubin SM, Dimitrov IE, Ruiz EJ, Wemmer DE, Pines A, Yao SQ, Tian F, Schultz PG. Proc. Natl. Acad. Sci., U.S.A 2001;98:10654–10657. [PubMed: 11535830]

3. Spence MM, Ruiz EJ, Rubin SM, Lowery TJ, Winssinger N, Schultz PG, Wemmer DE, Pines A. J. Am. Chem. Soc 2004;126:15287–15294. [PubMed: 15548026]

4. Wei Q, Seward GK, Hill PA, Patton B, Dimitrov IE, Kuzma NN, Dmochowski IJ. J. Am. Chem. Soc 2006;128:13274–13283. [PubMed: 17017809]

5. Hilty C, Lowery TJ, Wemmer DE, Pines A. Angew. Chem. Int. Ed 2006;45:70–73.

6. Schroder L, Lowery TJ, Hilty C, Wemmer DE, Pines A. Science 2006;314:446–449. [PubMed: 17053143]

7. Garcia S, Chavez L, Lowery TJ, Han S-I, Wemmer DE, Pines A. J. Mag. Res 2007;184:72–77.

8. Berthault P, Bogaert-Buchmann A, Desvaux H, Huber G, Boulard Y. J. Am. Chem. Soc 2008;130:16456–16457.

9. Hill PA, Wei Q, Eckenhoff RG, Dmochowski IJ. J. Am. Chem. Soc 2007;129:9262–9263. [PubMed: 17616197]

10. Aaron JA, Chambers JM, Jude KM, Costanzo LD, Dmochowski IJ, Christianson DW. J. Am. Chem. Soc 2008;130:6942–6943. [PubMed: 18461940]

11. Chambers JM, Hill PA, Aaron JA, Han Z, Christianson DW, Kuzma NN, Dmochowski IJ. J. Am. Chem. Soc. 2008

12. Branda N, Grotzfeld RM, Valdés C Jr, J R. J. Am. Chem. Soc 1995;117:85–88.

13. Brotin T, Dutasta JP. Eur. J. Org. Chem 2003;6:973–984.

14. Fogarty HA, Berthault P, Brotin T, Huber G, Desvaux H, Dutasta JP. J. Am. Chem. Soc 2007;12910332-+

15. Huber G, Beguin L, Desvaux H, Brotin T, Fogarty HA, Dutasta J-P, Berthault P. J. Phys. Chem. A 2008;112:11363–11372. [PubMed: 18925727]

16. Leontiev AV, Saleh AW, Rudkevich DM. Org. Lett 2007;9:1753–1755. [PubMed: 17394350]

17. Nakazawa J, Hagiwara J, Mizuki M, Shimazaki Y, Tani F, Naruta Y. Angew. Chem. Int. Ed 2005;44:3744–3746.

18. Scarso A, Pellizzaro L, Lucchi OD, Linden A, Fabris F. Angew. Chem. Int. Ed 2007;46:4972–4975.

19. Atwood JL, Barbour LJ, Jerga A. Science 2002;296:2367–2369. [PubMed: 12004074]

20. Enright GD, Udachin KA, Moudrakovski IL, Ripmeester JA. J. Am. Chem. Soc 2003;125:9896–9897. [PubMed: 12914432]

21. Brouwer DH, Moudrakovski IL, Udachin KA, Enright GD, Ripmeester JA. Crys. Growth Des 2008;8:1878–1885.

22. Dubes A, Moudrakovski IL, Shahgaldian P, Coleman AW, Ratcliffe CI, Ripmeester JA. J. Am. Chem. Soc 2004;126:6236–6237. [PubMed: 15149213]

23. Fielding L. Tetrahedron 2000;56:6151.

24. Wiseman T, Williston S, Brandts JF, Lin LN. Anal. Biochem 1989;179:131–137. [PubMed: 2757186]

25. Fisher HF, Singh N. Meth. Enzymol 1995;259:194–221. [PubMed: 8538455]

26. Kirby EP, Steiner RF. J. Phys. Chem 1970;74:4480–4490.

27. Darzac M, Brotin T, Bouchu D, Dutasta JP. Chem. Commun 2002:48–49.

28. Darzac M, Brotin T, Rousset-Arzel L, Bouchu D, Dutasta JP. New J. Chem 2004;28:502–512.

29. Brotin T, Dutasta J-P. Chem. Rev. 2008

30. Brotin T, Roy V, Dutasta JP. J. Org. Chem 2005;70:6187–6195. [PubMed: 16050676]

31. Kim BS, Ko YH, Kim Y, Li HJ, Selvpalam N, Lee HC, Kim K. Chem. Commun 2008:2756–2758.

32. Grabner G, Monti S, Marconi G, Mayer B, Klein C, Kohler G. J. Phys. Chem 1996;100:20068–20075.

33. Horrocks AR, Kearvell A, Tickle K, Wilkinso F. Trans. Faraday Soc 1966;62:3393–3399.

34. Lacowicz, JR. Principles of Fluorescence Spectroscopy. New York: Plenum Press; 1983.

35. Webber SE. Photochem. Photobio 1997;65:33–36.

36. Wolber J, Doran SJ, Leach MO, Bifone A. Chem. Phys. Lett 1998;296:391–396.

37. Hayes NV, Branch GEK. J. Am. Chem. Soc 1943;65:1555–1564.

38. Newman MS, Fukunaga T. J. Am. Chem. Soc 1963;85:1176–1178.

39. Harris, DC. Quantitative Chemical Analysis. New York: W. H. Freeman and Company; 1998.

40. Huber G, Brotin T, Dubois L, Desvaux H, Dutasta JP, Berthault P. J. Am. Chem. Soc 2006;128:6239–6246. [PubMed: 16669694]

41. Germain P, Letoffe JM, Merlin MP, Buschmann HJ. Thermochim. Acta 1998;315:87–92.

42. Canceill J, Lacombe L, Collet A. J. Chem. Soc. Chem. Commun 1987:219–221.

43. Collet, A. Comprehensive Supramolecular Chemistry. Atwood, JL.; MacNicol, DD.; Davis, JED.; Vogtle, F., editors. Vol. Vol. 2. New York: Pergamon; 1996. p. 325-365.

44. Clever, HL. Solubility Data Series. Vol. Vol. 2. New York: Pergamon Press; 1979.
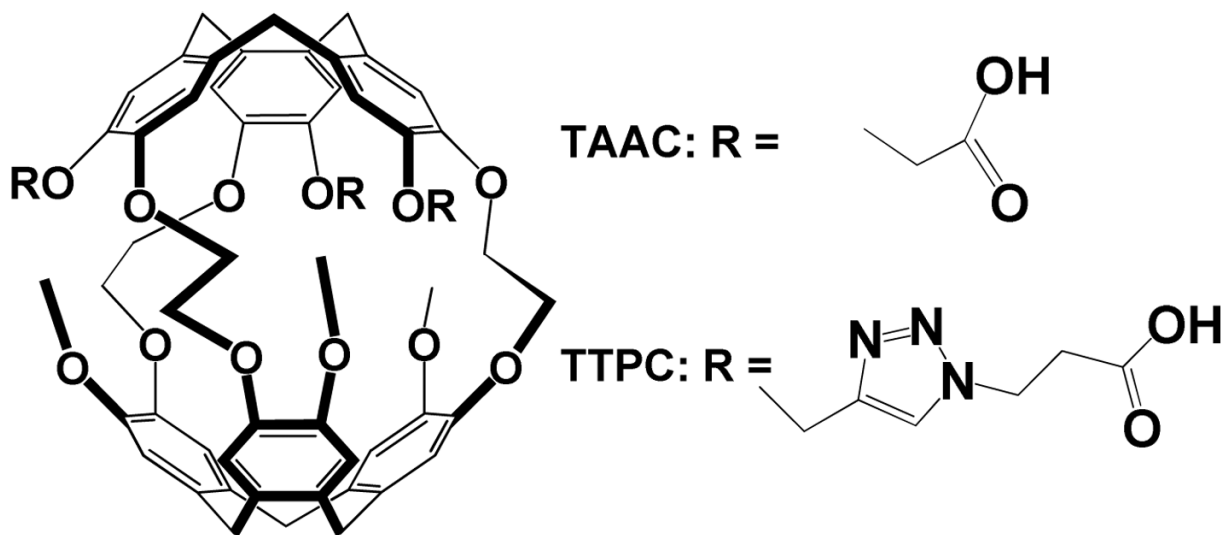
Figure 1.
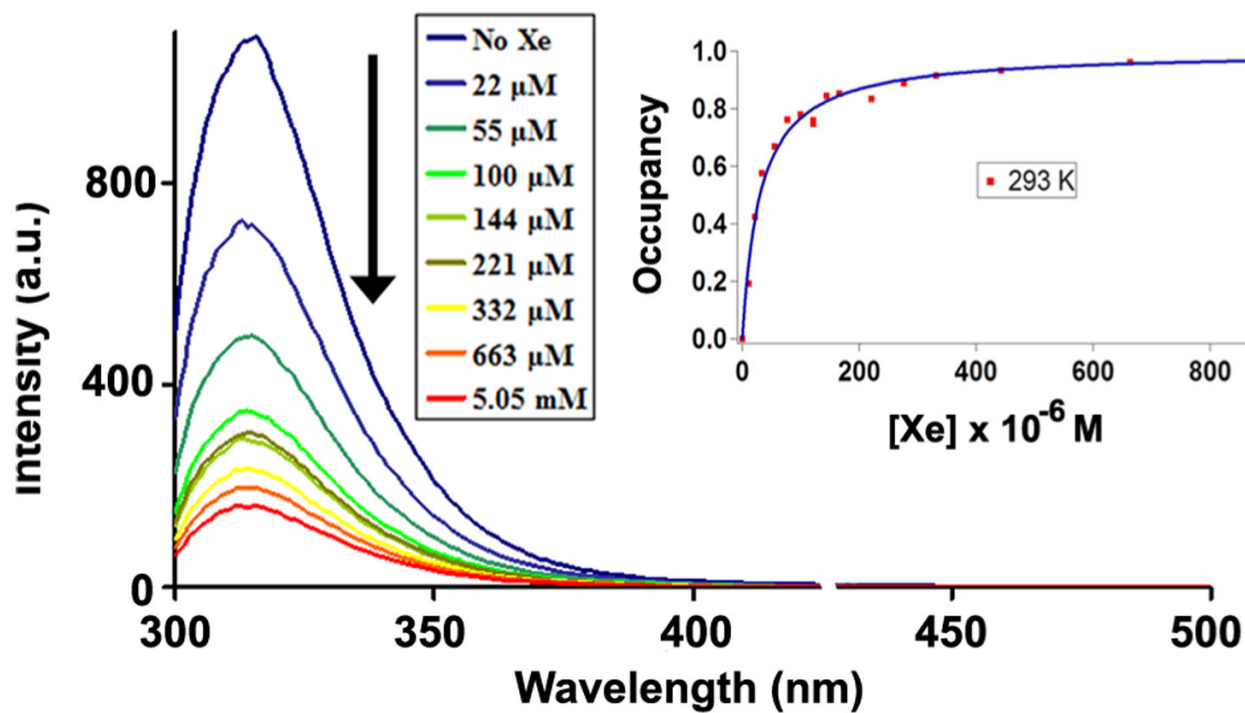Water-soluble cryptophanes **TAAC** and **TTPC**

Figure 2.
Fluorescence quenching of **TAAC** (15 µM) by Xe in 1 mM, pH 7.2 phosphate buffer, 293 K.
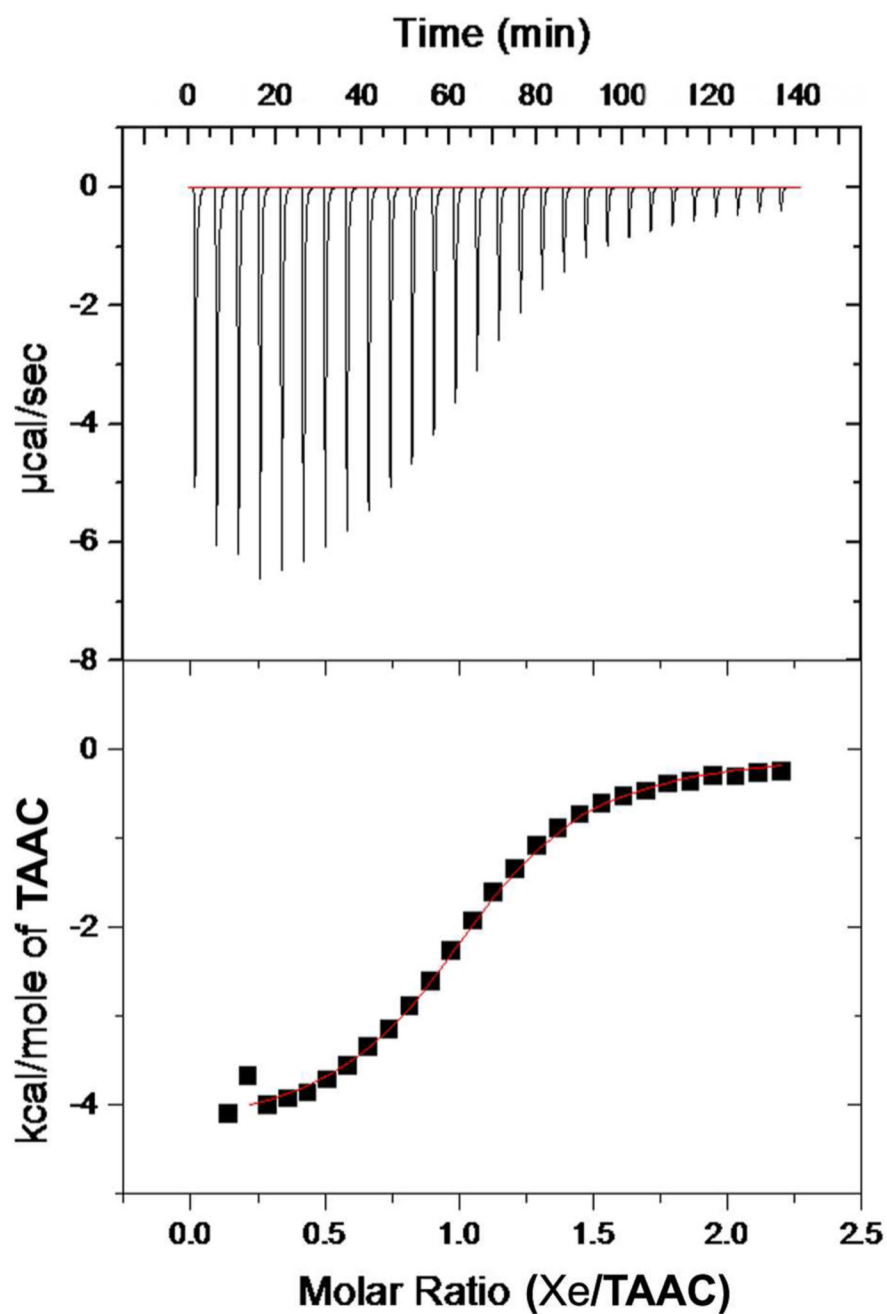Inset: Curve fit for a single-site binding model.

Figure 3.
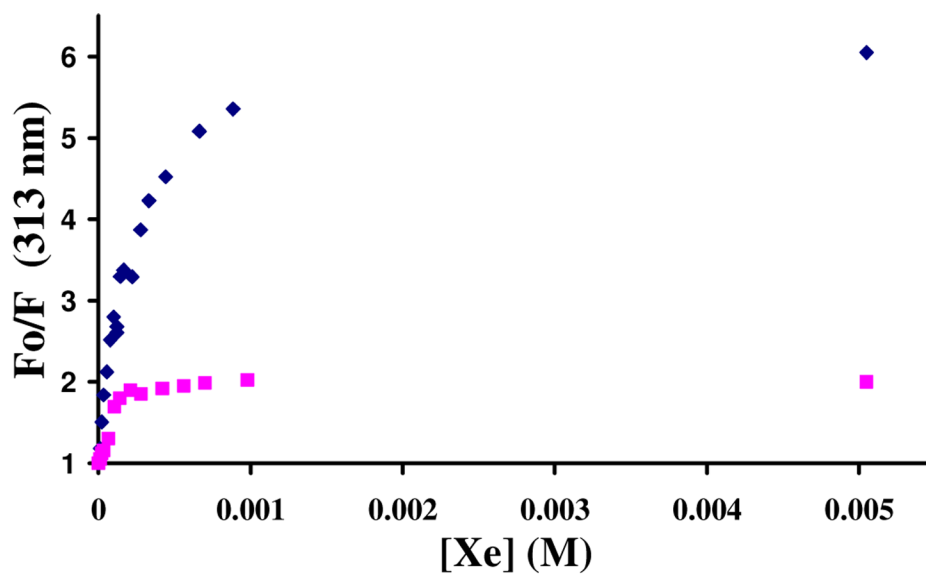Enthalpogram of 5.05 mM aqueous xenon solution titrated into 0.77 mM **TAAC** at 293 K.

Figure 4.
Stern-Volmer plots of fluorescence quenching by xenon of **TAAC** (blue diamonds) and **TTPC** (pink squares).
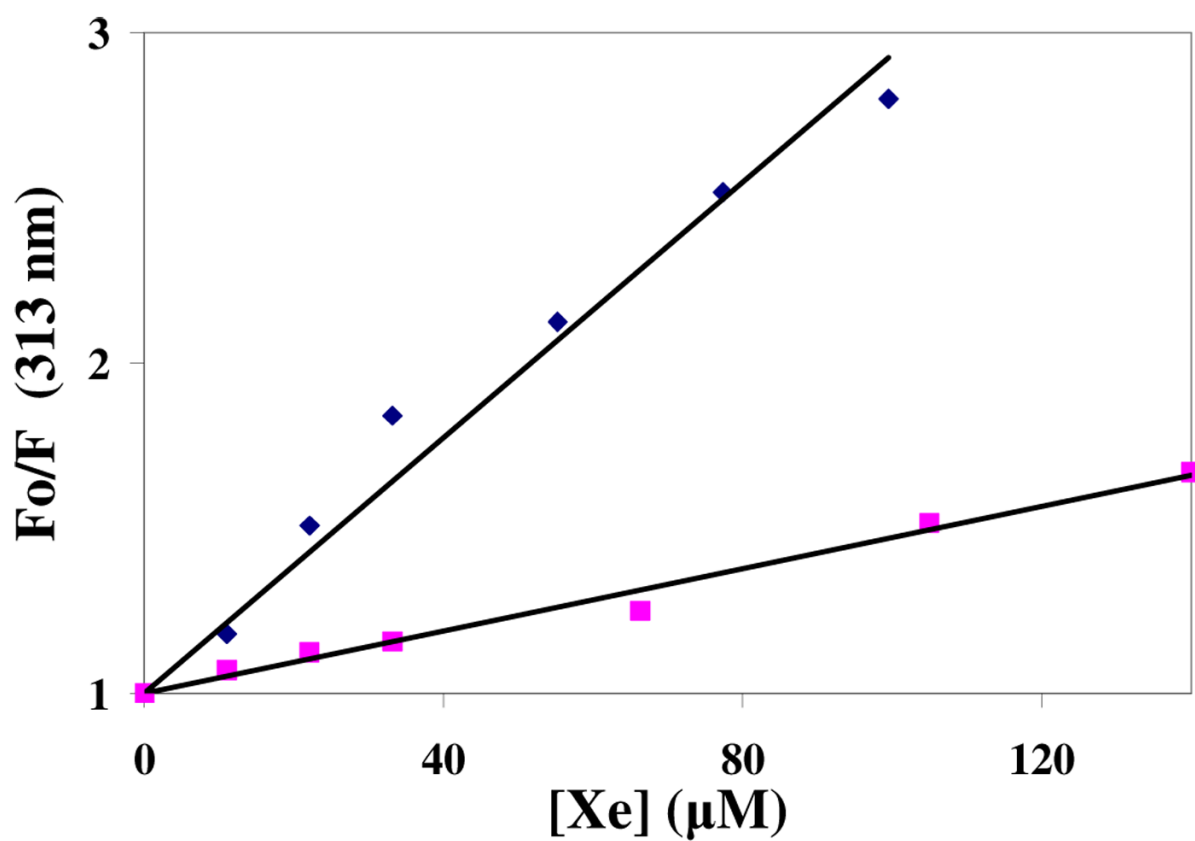
Figure 5.
Initial slopes of steady-state Stern-Volmer plots of **TAAC** (blue diamonds) and **TTPC** (pink squares).
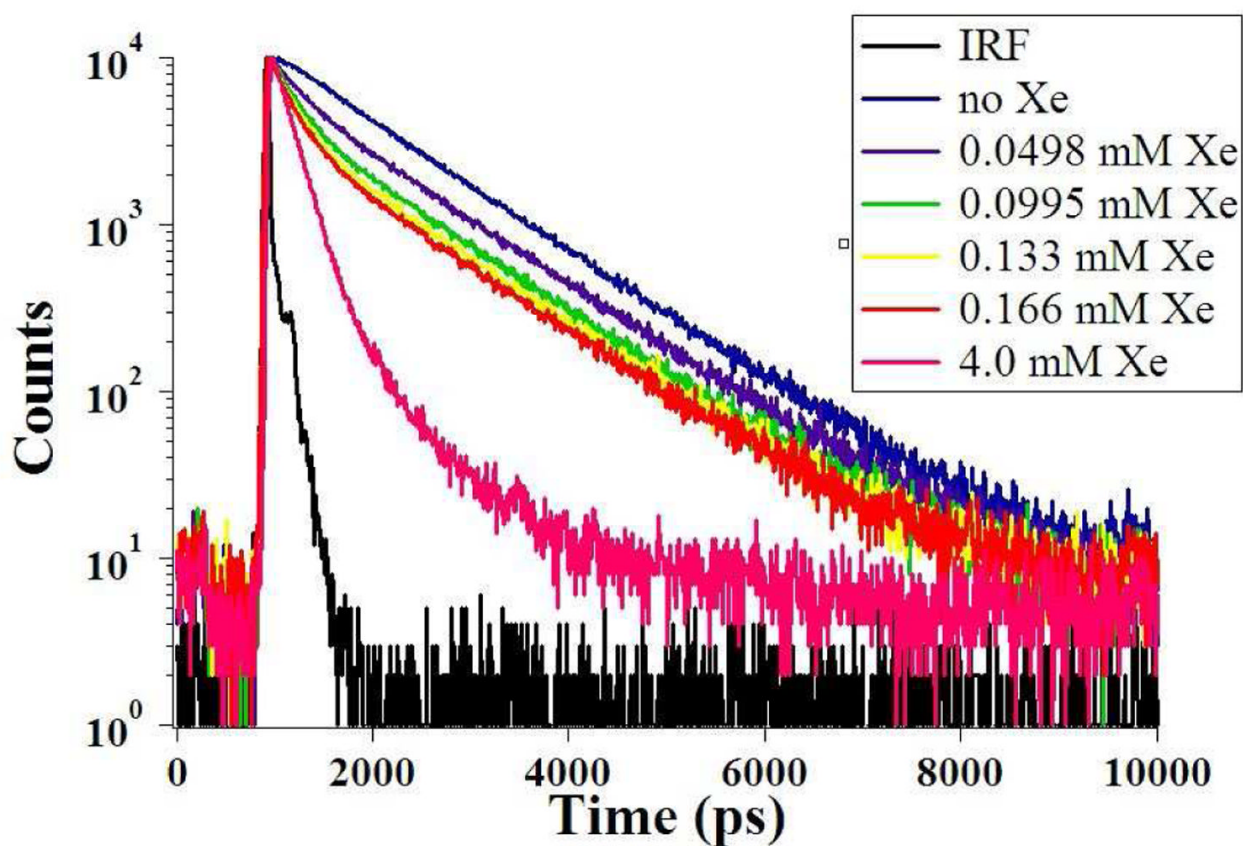
Figure 6.
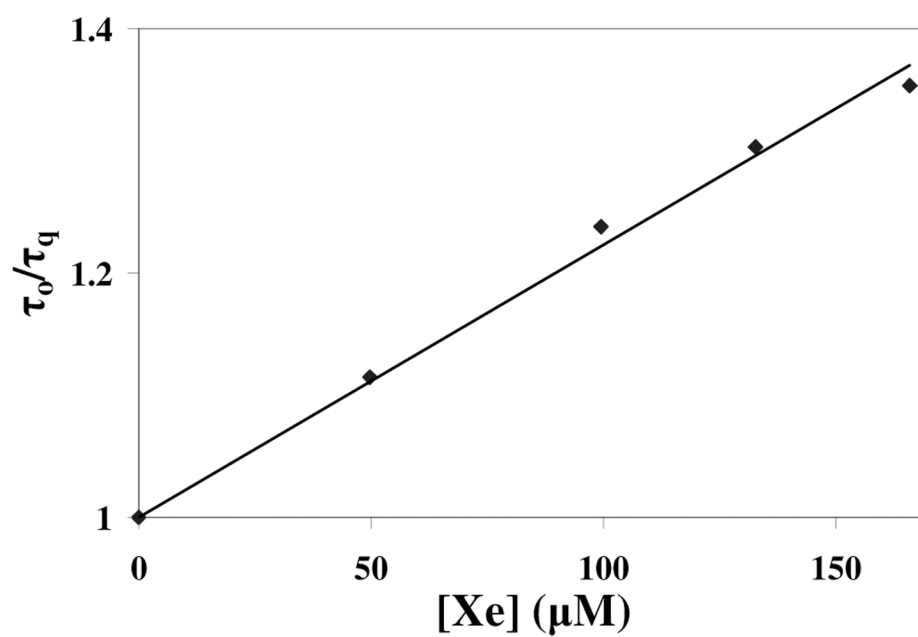Fluorescence decays of **TAAC** with increasing amounts of xenon and the deconvolved instrument response function (IRF).

Figure 7.
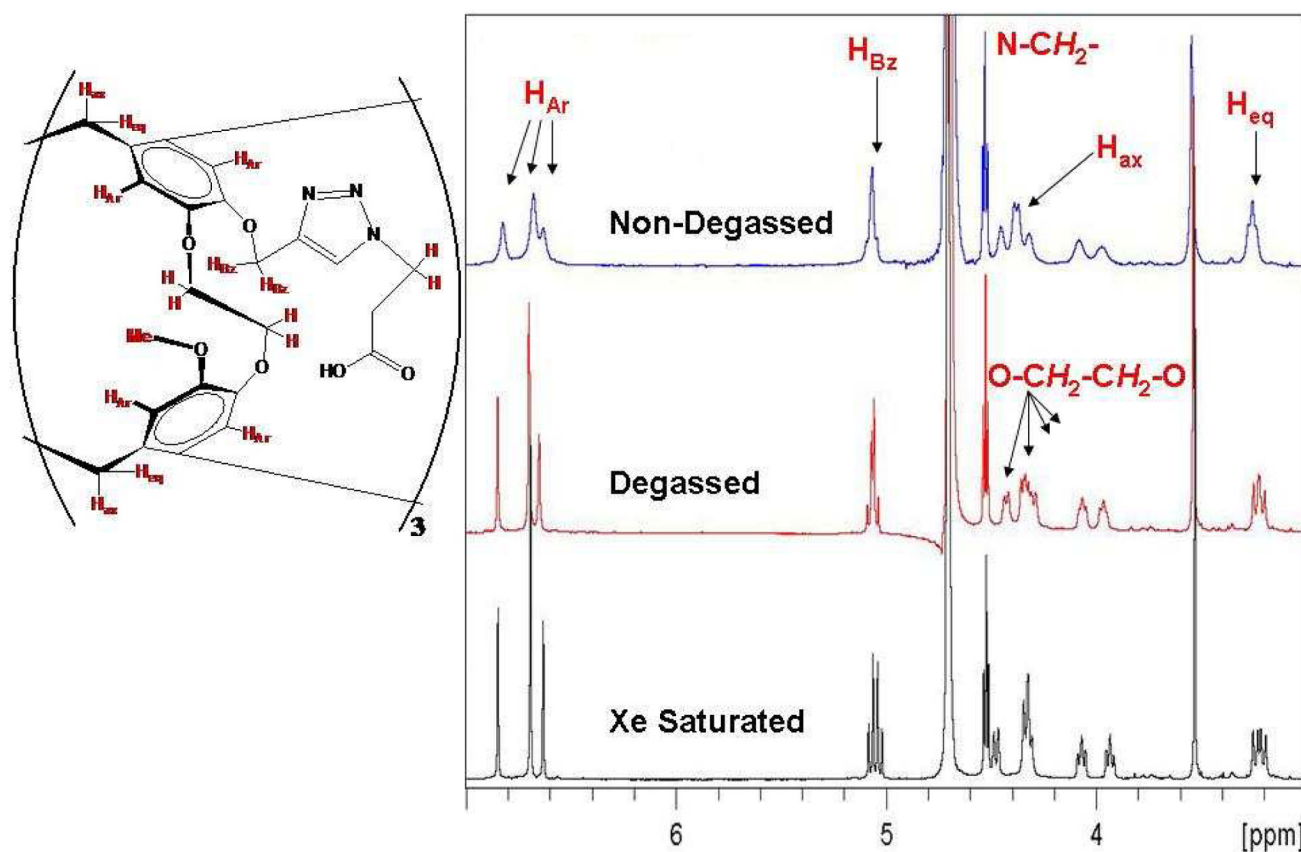Initial slope of time-resolved Stern-Volmer plot of **TAAC**.

Figure 8.
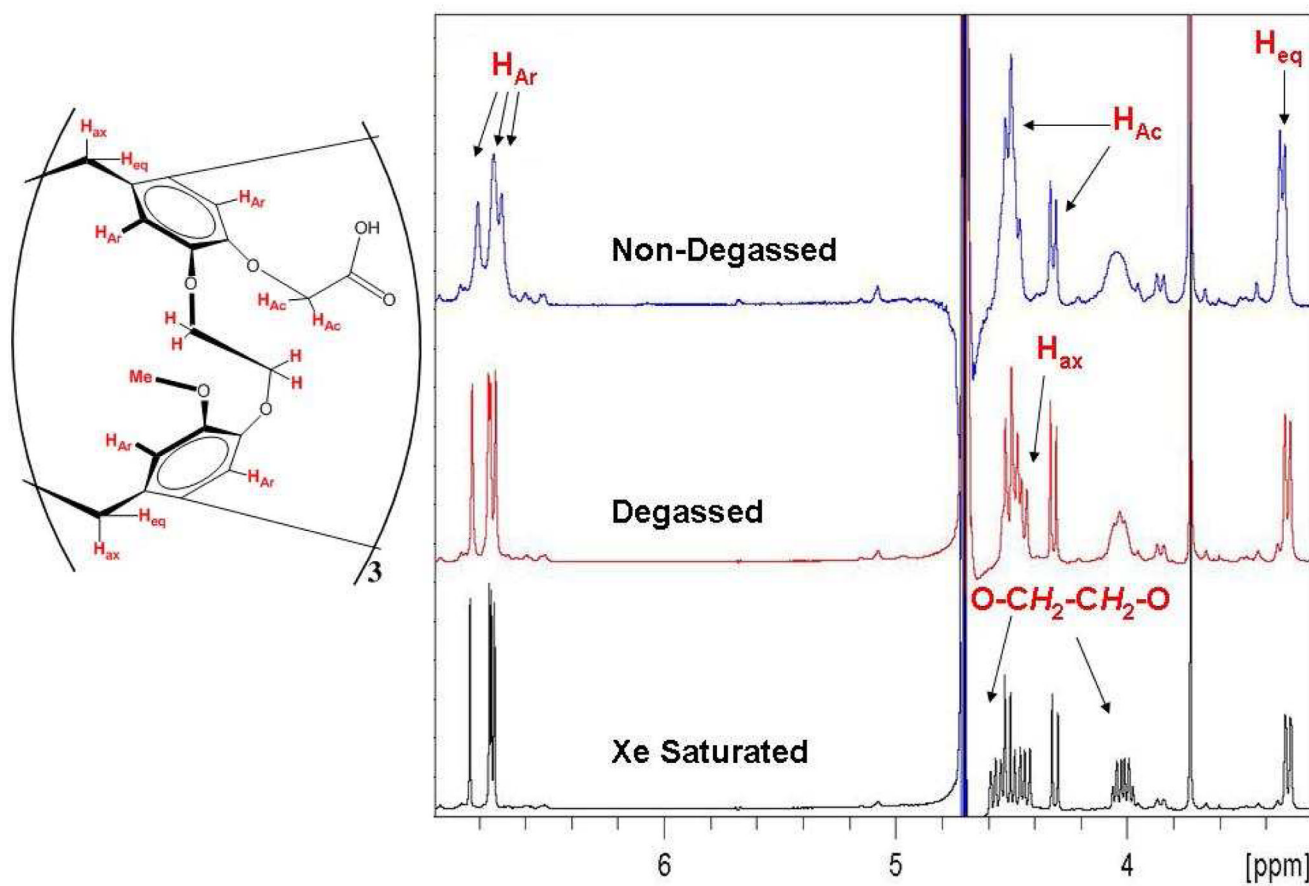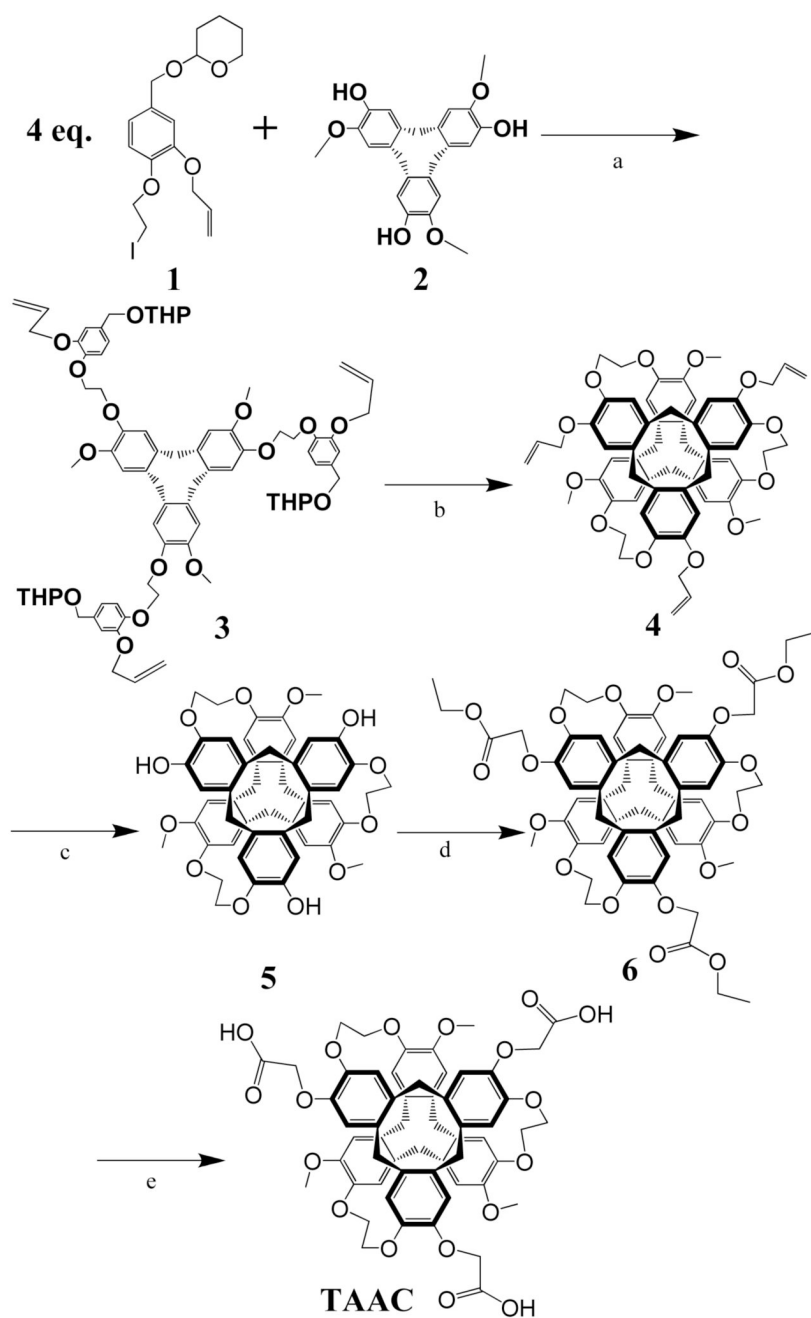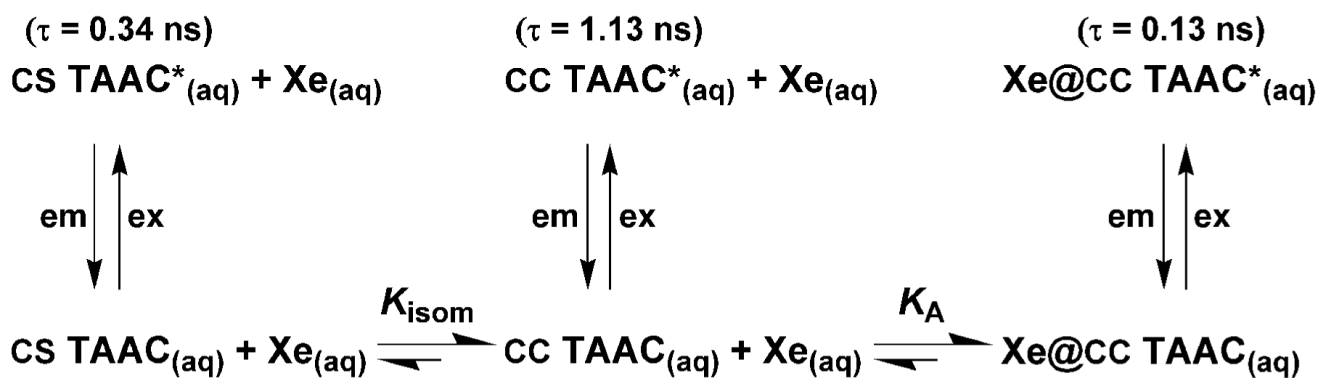600 MHz ^{1}H NMR spectrum of **TTPC** in 10% D_2O.

Figure 9.
600 MHz ^{1}H NMR spectrum of **TAAC** in 10% D_2O.

Scheme 1.

13-step synthesis of water-soluble triacetic acid cryptophane **TAAC**[*]

[*]Conditions: (a) Cs_2CO_3, DMF, 55 °C, 12 h, 60%; (b) $CHCl_3$, HCOOH, reflux, 9 h, 40%; (c) $Pd(OAc)_2$, $P(Ph)_3$, $(Et)_2NH$, THF, H_2O, 80 °C, 4 h, 84%; (d) ethylbromoacetate, Cs_2CO_3, DMF, 60 °C, 12 h, 79%.; (e) KOH (2 M), THF, 70 °C, 12 h, 87%.

$(\tau = 0.34 \text{ ns})$

CS TAAC$^{*}_{(aq)}$ + Xe$_{(aq)}$

$(\tau = 1.13 \text{ ns})$

CC TAAC$^{*}_{(aq)}$ + Xe$_{(aq)}$

$(\tau = 0.13 \text{ ns})$

Xe@CC TAAC$^{*}_{(aq)}$

em | ex

em | ex

em | ex

$$\text{CS TAAC}_{(aq)} + \text{Xe}_{(aq)} \xrightleftharpoons{K_{isom}} \text{CC TAAC}_{(aq)} + \text{Xe}_{(aq)} \xrightleftharpoons{K_A} \text{Xe@CC TAAC}_{(aq)}$$

Scheme 2.
Proposed model of fluorescence quenching of **TAAC** by encapsulated xenon. The excitation
(ex) and emission (em) wavelengths are 280 nm and 313 nm, respectively.

Table 1

Reaction times and yields for formation of tri-allyl cryptophane **4**.

Solvent	Temp (°C)	Time (h)	Yield
HCOOH, $CHCl_3$	55	2.5	0%
HCOOH, $CHCl_3$	reflux	3	17%
HCOOH, $CHCl_3$	reflux	6	32%
HCOOH, $CHCl_3$	reflux	9	40%
HCOOH, $CHCl_3$	reflux	22	25%
HCOOH, $Cl(CH_2)_2Cl$	reflux	1	decomp

Table 2

Thermodynamic binding parameters of Xe@**TAAC** obtained by ITC at 293 K

Cryptophane	K_A (M^{-1}×10^4)	ΔG (kcal mol^{-1})	ΔH (kcal mol^{-1})	TΔS (kcal mol^{-1})
TAAC	3.33 ± 0.28	−6.06	−4.34 ± 0.66	1.72
TTPC[a]	1.70 ± 0.17	−5.69	−3.14 ± 0.20	2.55

[a] previously reported values[9]

Table 3

Results of a three-exponential global fit of the lifetime data of **TAAC** with increasing concentrations of xenon

[Xe] mM	Avg τ	$I_{1.13 \text{ ns}}$	$I_{0.344 \text{ ns}}$	$I_{0.134 \text{ ns}}$
0.000	1.09	0.95	0.05	0.0
0.05	0.98	0.83	0.08	0.10
0.10	0.88	0.73	0.10	0.17
0.13	0.84	0.68	0.12	0.20
0.17	0.80	0.65	0.13	0.23
4.00	0.24	0.05	0.24	0.71